Doppler-Shift Attenuation Measurements of Lifetimes for $(2s, 1d)$-Shell Nuclei Excited by Heavy-Ion Bombardment of $^2H^\dagger$

E. K. Warburton, J. W. Olness, G. A. P. Engelbertink,* and T. K. Alexander‡
Brookhaven National Laboratory, Upton, New York 11973
(Received 8 September 1972)

The Doppler-shift attenuation method was used to measure the lifetimes of nuclear levels formed in the heavy-ion bombardment of titanium deuteride targets. The nuclei formed are those resulting from the "inverse" (d,p) and (d,n) reactions, using beams of ^{18}O, ^{19}F, ^{32}S, ^{34}S, ^{35}Cl, and ^{37}Cl. Target backings of Mg, Al, and Cu were used as stopping media for the γ-decaying nuclei. γ rays were observed, mostly at 0° to the beam, with a 35-cm^3 Ge(Li) detector. New results include mean lifetimes of 1.8 ± 0.34 psec for the ^{33}Cl 811-keV level, 3.3 ± 0.5 psec for the ^{35}S 1574-keV level, and 1.50 ± 0.18 psec for the 2468-keV level of ^{36}Cl. The advantages and limitations of the method are discussed.

I. INTRODUCTION

Study of the Doppler effects associated with the emission of γ radiation from nuclei recoiling after a nuclear reaction has become the most widely used method of determining the lifetimes of nuclear levels.[1] The method can be said to have reached maturity when the experimental techniques were developed to the point that the γ-ray energy resolution of the detecting system was smaller than, or at least comparable to, the energy shift due to the Doppler effect. The energy of the γ rays emitted at an angle θ relative to the direction of motion of a nucleus traveling at velocity $v(t) = c\beta(t)$ is, to second order in $\beta(t)$,

$$E_\gamma = E_{\gamma 0}[1 + \beta(t)\cos\theta - \tfrac{1}{2}\beta(t)^2 + \beta(t)^2\cos^2\theta], \quad (1)$$

where $E_{\gamma 0}$ is the energy of the γ rays emitted by nuclei at rest. In most practical applications the second-order terms are essentially negligible, and the Doppler shift is very nearly proportional to the nuclear velocity. Therefore, the detector energy resolution must be smaller than, or comparable to, the product $E_{\gamma 0}\beta(0)$. The first type of Doppler-shift study for which this situation could be routinely achieved utilized heavy-ion bombardment of light targets, a type of reaction which for convenience we shall label an "inverse" reaction. By means of such reactions relatively large Doppler shifts are produced. In the first comprehensive study of this type, Litherland, Yates, Hinds, and Eccleshall[2] used the ^{16}O bombardment of ^3H to produce recoiling ^{18}O and ^{18}F ions with velocities $\beta \simeq 0.05$, some $\frac{16}{3}$ larger than would be obtained for ^3H bombardment of ^{16}O at the same center-of-mass energy. They used NaI(Tl) detectors which have a nominal 6% energy resolution for 1-MeV γ rays. Soon after their report appeared in 1963, the Ge(Li) detector became available for Doppler-shift studies, with an energy resolution ~25 times better than that of NaI(Tl) detectors, e.g., for 1-MeV γ rays the resolution figures are ~2.5 keV for Ge(Li) as opposed to ~60 keV for NaI(Tl). The appearance of Ge(Li) detectors revolutionized the field, and technical developments for the Doppler-shift attenuation method (DSAM) in the years since 1963 have been largely connected with the utilization of those detectors in "normal" reactions.

Nevertheless, some use of "inverse" reactions has continued and the advantages and disadvantages of this technique have become clearer. The two obvious advantages of inverting the "normal" reaction result from the production of a larger Doppler shift and a decrease in the percentage spread in velocity. For example, in a reaction of the type $M_2(m_1, m_4)M_3^*$ initiated with a beam of particles m_1 at a laboratory energy E_1, the z component of velocity for the excited nuclei M_3^* at the moment of formation $(t = 0)$ is

$$\beta_z(0) = \beta_{\text{c.m.}}(1 + \gamma^{-1}\cos\theta_{\text{c.m.}}), \quad (2)$$

where the first term is the velocity of the center of mass and the second is the velocity of M_3^* in the center-of-mass system and $\theta_{\text{c.m.}}$ is the center-of-mass angle of M_3^*. For the same energy in the center of mass, i.e., the same E/M for the beam, reversing the roles of m_1 and M_2 multiplies $\beta_{\text{c.m.}}$ by M_2/m_1 and leaves $\beta_{\text{c.m.}}\gamma^{-1}$, the velocity of M_3^* in the c.m. system, unchanged. To illustrate, consider the production of the 1617-keV level of ^{38}Cl by the interaction of ^{37}Cl and ^2H. For the $^{37}Cl(d,p)^{38}Cl$ reaction[3] leading to the 1617-keV level at $E_d = 3.24$ MeV we have

$$\beta_z(0) = 0.00303\ (1 + 0.919\cos\theta_{\text{c.m.}})$$

for

$$E_d/2 = 1.62\ \text{MeV}.$$

It is clear that the recoiling nuclei do not approximate a unidirectional, monoenergetic beam. On the other hand, for the inverse reaction initiated by 60-MeV ^{37}Cl ions we have

$$\beta_z(0) = 0.056(1 + 0.0497\cos\theta_{\text{c.m.}})$$

for

$$E_{\text{Cl}}/37 = 1.62 \text{ MeV},$$

and the maximum spread in $\beta_z(0)$ is ±5%, while the maximum half angle of the cone of recoiling ^{38}Cl nuclei {given by $\cos^{-1}[(1-\gamma^{-2})^{1/2}]$} is 2.8° as opposed to 67° for the "normal" reaction. In the example chosen, then, the ^{37}Cl bombardment produces an ensemble of ^{38}Cl nuclei with about 10 times the velocity that would result if the same angular spread of ±2.8° about the z axis were selected by coincidence detection of the protons in the ^{37}Cl$(d,p)^{38}$Cl reaction. Since the intrinsic line width of the Ge(Li) detector is much less than the full Doppler shift, the detailed line shapes resulting from the velocity distribution of decaying recoil nuclei are obtained and are not obscured by the detector resolution. However, the broad line shapes can give rise to difficulties due to background and overlapping γ rays.

A third advantage of heavy-ion bombardments is that there is more freedom in choosing the backing material in which the recoiling nuclei are slowed down. This is true since the backgrounds due to nuclear reactions induced in the backing are usually less troublesome for heavy-ion bombardment than for light-particle bombardment. For example, the use of magnesium backings as in the ^{3}H$(^{16}$O$,p)^{18}$O and ^{3}H$(^{16}$O$,n)^{18}$F work of Litherland *et al.*[2] would not have been feasible in the inverse reactions, since ^{24}Mg + ^{3}H is a prolific source of γ rays. In general, for targets of the hydrogen isotopes the background is usually considerably reduced relative to the "normal" reaction, since in the latter case ^{1}H, ^{2}H, and ^{3}H beams produce γ rays in the beam defining and stopping materials as well as in the target and target backing.

A fourth advantage of the inverse reaction, assuming as always the same center-of-mass energy, is that the much larger ranges involved (as a rough rule of thumb, range is proportional to velocity) means that the fractional energy loss in the target material can be considerably reduced, thus reducing uncertainties due to the finite target thickness or to surface effects. This means that one also has a wider choice of stopping media for the recoiling ion, and further, that the results will be less sensitive to local voids and disturbances in the stopping media. In particular, we avoid the constraint of being forced to use the same evaporated compound for both target and stopping media, often encountered when using "normal" reactions yielding low recoil velocities.

A fifth advantage also stemming from the high recoil velocities is that for $\beta > 1\%$, our present knowledge of the stopping power of heavy ions is more reliable and more widely investigated (see Northcliff and Schilling,[4] for instance), since the higher energies involved render dE/dx measurements easier, and since the main contribution to the stopping is the electronic stopping process, as opposed to the situation for lower velocities where nuclear stopping, which is difficult to treat and not well investigated, is important.

The "inverse" reaction lends itself well to fast surveys in which the principal motive is to gain information for the planning of future work. An example from the present work is the ^{2}H$(^{35}$Cl$,p)^{36}$Cl reaction. There was no information at all on the lifetimes of the low-lying states of ^{36}Cl when this work was started. Thus it was not known whether the recoil distance technique[1] or the DSAM, or some other technique, was most suitable for measuring the lifetimes of, say, the first two levels of ^{36}Cl. This question was answered from a few hours accumulation of the γ-ray spectra from ^{2}H + ^{35}Cl.

This, then, is a report of the results of a survey of the Doppler-shift information obtained from the bombardment of ^{2}H with various ions accelerated at the Brookhaven National Laboratory (BNL) MP-tandem Van de Graaff facility.

The next section (Sec. II) contains a brief description of the experimental method; Sec. III describes the method of analysis; the results are presented in Sec. IV; and in Sec. V we discuss these results and limitations of the method.

II. EXPERIMENTAL METHOD

The targets were prepared by evaporating titanium onto the target backings in a deuterium atmosphere. The backings were carefully cleaned blanks of copper, aluminum, and magnesium. In order to check that the ^{2}H was absorbed in the titanium and not the backings, the latter were checked for ^{2}H by heavy-ion bombardment of the reverse sides. No ^{2}H was detectable. The nominal titanium thickness of 200 μg/cm^2 was believed accurate to about 10%. The density was assumed to be that of titanium metal (4.52 g/cm^3) as opposed to that for titanium "deuteride" (TiD) which for the maximum possible deuterium content[5] has a density of 3.99 g/cm^3. In all the present measurements the energy loss in the targets was almost negligible. For instance, the ^{32}S ions in the ^{2}H + ^{32}S measurements have 97.9% of their original

velocity after penetrating the TiD. Thus, any uncertainty in these assumptions about the target composition has only a negligible effect on the lifetimes derived.

The present survey was carried out during the first summer (1970) of operation of the BNL MP-tandem Van de Graaff facility and, therefore, it was made in conjunction with development of the ion source capabilities of the installation. Thus, the measurements were kept simple and of short duration so that for some cases the statistics are less than desirable. The main characteristics of these studies are given in Table I, which lists the six beams used, the charge state selected, and the final beam energy and intensity. Only for the case of the ^{34}S beam, which was extracted from natural sulphur (4.22% ^{34}S), was the beam intensity limited by the ion source. In all other cases it was limited by the requirement that the heating of the target or the detector counting rate be held within acceptable limits. The beam energy was chosen as low as possible commensurate with a reasonable cross section. The equivalent deuteron energy for the same center-of-mass energy is listed in column 5 of Table I.

A 35-cm^3 Ge(Li) detector with a full width at half maximum (FWHM) of 2 keV for 656-keV γ rays was used throughout. The detector-target distance (see Table I) was kept as small as possible without introducing appreciable error into the evaluation of the Doppler shift for $\theta = 0°$. As will be discussed, the finite angle subtended by the detector does have appreciable effect on such measurements for $\theta \gtrsim 45°$. The targets were bombarded in a simple target holder fabricated from a test tube. There was no target cooling. Spectra were recorded in a 4096-channel analyzer. In all cases the energy calibration of the spectra was internal; that is, there were enough radioactive γ ray lines of accurately known energies to provide a calibration. Examples are the ground-state decay of the low-lying states of $^{46,48}Ti$, ^{24}Mg, ^{27}Al, and $^{63,65}Cu$ from Coulomb excitations of the target and backing materials.

III. ANALYSIS

A. γ-Ray Spectra

Standard techniques[6] of data reduction were employed to calibrate the γ-ray spectra, using those peaks for which the energies were well known. Likewise, the backgrounds under the γ-ray line shapes were subtracted by least-squares-fitting an exponential function to the regions on either side of a given peak. In some cases this was not adequate because the background had structure. Such cases will be discussed individually in the next section.

B. Energy Loss Parametrization

The energy loss of the recoiling ions in the target and backing material was assumed to consist of a nuclear part, $(dE/dx)_n$, most important at low velocities near the end of the ion range and giving rise to large-angle scattering, and an electronic part, $(dE/dx)_e$, which gives rise to negligible changes in direction and is by far the more important for the velocities used in the present work. What is actually needed in the present work is dv_z/dt, which is related (nonrelativistically) to dE/dx, if we assume no change in direction, by $M dv_z/dt = dE/dx$. Because of the nuclear scattering the relationship is not so simply obtained in practice. We use the parametrization

$$M\frac{dv_z}{dt} = \left.\frac{dE}{dx}\right|_n + \left.\frac{dE}{dx}\right|_e . \tag{3}$$

TABLE I. Beam and detection characteristics for the six heavy-ion beams. The equivalent deuteron energy corresponding to the same c.m. energy in the "inverse" reaction is indicated.

Ion	Charge state	Beam Energy (MeV)	Intensity (nA)	E_d (MeV)	Detector Distance (cm)	Time [a] (h)	θ [b] (deg)
^{18}O	4^+	26.2	100	2.76	7.0	2.0	0, 30, 60, 90
^{19}F	4^+	24.6	200	2.59	7.5	2.0	0, 60, 90, 120
^{32}S	6^+	54.6	200	3.41	6.0	2.0	0, 45, 90
^{34}S	6^+	59.6	70	3.51	10.0	3.0	0, 55, 90, 120
^{35}Cl	6^+	57.4	100	3.28	6.0	2.0	0, 55, 90
^{37}Cl	6^+	57.4	130	3.48	6.0	2.5	0, 55, 90

[a] The *average* time to collect each of the various spectra.
[b] Of the three targets available, not all were used at each angle listed.

We assume that the electronic energy loss process gives rise to negligible directional change, and that the nuclear stopping and scattering can be parametrized as $-(dE/dx)_n = K_n/(v/v_0)$, where $v_0 = c/137$. The parameter K_n can be estimated by fitting[7,8] projected range data, or in the absence of specific data, a good approximation can be obtained[8] by setting K_n equal to Bohr's estimate[8,9] of $-(dE/dx)_n$ at $v/v_0 = 1$. Our results are largely insensitive to K_n; for example, varying K_n by a factor of 2 produces a change of less than 10% in any of the lifetimes extracted from our data.

In the present work, all available measurements of dE/dx for the recoiling ions and backing materials were utilized in an effort to obtain the best possible description of the electronic energy loss. The most useful data were those of Porat and Ramavataram[10] for oxygen and other light ions stopping in Al and Ni, and of Booth and Grant[11] for oxygen and chlorine ions stopping in Al and Ni. The electronic part of dE/dx for the ion and stopping-media combinations used in the present investigation were interpolated from these various experimental data using the systematics of the McMaster[12] and Aarhus[13] groups for $v/v_0 \lesssim 2$, and the effective charge concept[4,10,14,15] for $v/v_0 \gtrsim 2$.

The electronic energy loss data so obtained were fitted with the analytical functions:

$$-\left.\frac{dE}{dx}\right|_e = K_e\left(\frac{v_z}{v_0}\right) - K_3\left(\frac{v_z}{v_0}\right)^3, \qquad v_z/v_0 < v_c/v_0 \qquad (4a)$$

$$-\left.\frac{dE}{dx}\right|_e = A + B\left(\frac{v_z}{v_0}\right) - C\left(\frac{v_z}{v_0}\right)^2, \qquad v_z/v_0 \geq v_c/v_0 . \qquad (4b)$$

The parameters K_3 and v_c/v_0 were chosen so that $dE/dx|_e$ and its derivative were continuous at v_c/v_0. The resultant $M dv_z/dt$ was then obtained from Eq. (3) for $v_z < v_c$ and was assumed equal to $dE/dx|_e$ for $v_0 \geq v_c$. The parameters of Eqs. (3) and (4) for the ions and stopping materials used in the present work are listed in Table II. An example of a fit of Eq. (4) to experimental electronic energy loss data is shown in Fig. 1. It is estimated that the parameters of Table II, when used with Eqs. (3) and (4), give $M dv_z/dt$ to better than 10% for $v/v_0 > 2$.

For the parametrization of Eq. (4b), the line shape is given by

$$\frac{dN(V)}{dV} = N(0)\,x\left(\frac{\gamma_+}{\gamma_-}\right)^x \frac{\gamma_+ - \gamma_-}{(\gamma_+ + V)^2}\left(\frac{\gamma_- + V}{\gamma_+ + V}\right)^{x-1} \qquad (5)$$

for $-M dv_z/dt = A + B(v_z/v_0) - C(v_z/v_0)^2$, where $v(0)$ is the initial ion velocity, A, B, C are positive numbers, and

$$V = v_z(t)/v(0),$$

$$x = \alpha_2/\tau,$$

$$\alpha_2 = M v_0/Q,$$

$$Q = (B^2 + 4AC)^{1/2},$$

$$\gamma_\pm = -[v_0/v(0)](B \pm Q)/2C.$$

The line shape for $-M dv_z/dt = K_n(v_z/v_0)^{-1} + K_e(v_z/v_0) - K_3(v_z/v_0)^3$ has been given previously.[8] For the dE/dx of Eq. (4b), the fraction of nuclei remaining in the excited state of lifetime τ at any fractional

TABLE II. Parameters for the energy loss of ions in Mg, Al, and Cu. The parametrization is given in the text.

Ion	Stopping material	K_n [a]	K_e	K_3	v_c/v_0	A	B	C
Oxygen	Mg	0.206	3.022	0.084	3.225	4.436	1.145	0.115
	Al	0.189	2.780	0.077	3.151	3.657	1.225	0.118
	Cu	0.140	1.477	0.024	3.814	1.124	1.238	0.107
Flourine	Mg	0.248	2.622	0.030	5.155	2.942	2.140	0.194
	Al	0.233	2.448	0.031	4.731	2.336	2.164	0.193
	Cu	0.172	1.403	0.014	5.048	1.000	1.374	0.106
Sulfur	Mg	0.696	4.350	0.046	4.497	1.000	4.841	0.367
	Al	0.657	4.070	0.043	4.464	1.000	4.480	0.334
	Cu	0.492	2.520	0.022	4.655	1.000	2.572	0.161
Chlorine	Mg	0.788	4.800	0.059	3.993	2.468	4.507	0.317
	Al	0.744	4.340	0.050	3.829	0.908	4.595	0.319
	Cu	0.563	2.600	0.013	5.500	1.500	3.200	0.230

[a] This is the only parameter which depends on the atomic weight of the stopping ion. The numbers given are for ^{19}O, ^{20}F, ^{33}S, and ^{38}Cl.

velocity V is given by

$$N(V)=\left[\left(\frac{\gamma_-+V}{\gamma_++V}\right)\left(\frac{\gamma_++1}{\gamma_-+1}\right)\right]^x . \quad (6)$$

Note that the $N(0)$ of Eq. (5) is obtained by setting $V=0$ in Eq. (6). The procedure used to calculate the total line shape was to assume a *mean* range in the target corresponding to one half the target thickness. $dN(V)/dV$ was then calculated from $V=1$ to $V=V_T$ using the target material stopping parameters, where V_T is the fractional velocity at which the ions enter the backing material; the calculation of $dN(V)/dV$ from V_T to $V_c[\equiv v_c/v(0)]$ used the stopping parameters of the backing material. Finally $dN(V)/dV$ was calculated for $V \leq V_c$ using Eq. (B14) of Ref. 8. The normalization of $dN(V)/dV$ at the joining velocities V_T and V_c was accomplished with Eq. (6).

In several cases the line shape being studied was a function of more than one lifetime, since the level of mean life τ_1 emitting the γ rays in question was itself partially fed by the decay of a higher-lying level with a measurable lifetime τ_2. In this case the modification of Eqs. (5) and (6) was made by separation of variables:

$$\frac{dN(V)}{dV}=\frac{dN(V)}{dt}\,\frac{dt}{dV}, \quad (7)$$

which separates the well-known radioactive decay dN/dt, which is independent of Mdv_z/dt, from dt/dV which is obtained from Mdv_z/dt.

Before fitting to the experimental data, the theoretical line shape was convoluted with a detector-response function and with a function which approximated the experimental distribution of initial velocities. The detector response was assumed to be a Gaussian peak with a low-energy tail of constant amplitude. The tail intensity was determined from fits to monoenergetic calibration spectra, and corresponded to a counting rate (per channel) of ~1% of the Gaussian peak counting rate.

The finite target thickness, the kinematic effects of the reaction angular distribution, and the finite detector size, all introduce a spread in $V(0)\cos\theta$. For a target-to-detector distance of $h=7$ cm, for example, this spread was approximated by a Gaussian with a FWHM varying from 13% of V for a detector angle of 0°, to ~60%, at 60°. The variation with detector angle is caused by the $\cos\theta$ dependence of ΔV so that for the detector acceptance angle of 26°, for $h=7$ cm, $\Delta(\cos\theta)$ and thus ΔV are only 1.5% at $\theta=0°$, but are 40% at $\theta=60°$. For a spread of only 13% in V, the Gaussian smearing is probably not a bad approximation. However, for a spread of 60% in V the approximation is not adequate. Thus, the data for $\theta \leq 45°$ were mainly of qualitative use, with the main function of aiding

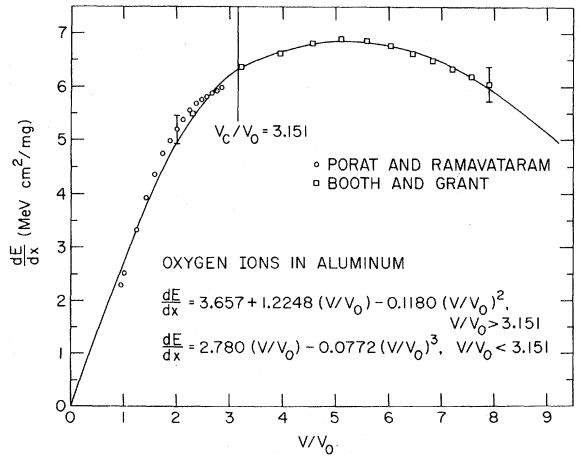

FIG. 1. The electronic stopping power for oxygen ions in ^{27}Al. The open circles and squares are experimental data from Refs. 10 and 11, respectively. 5% error bars are illustrated. The solid curve is the parametrization used in the present work.

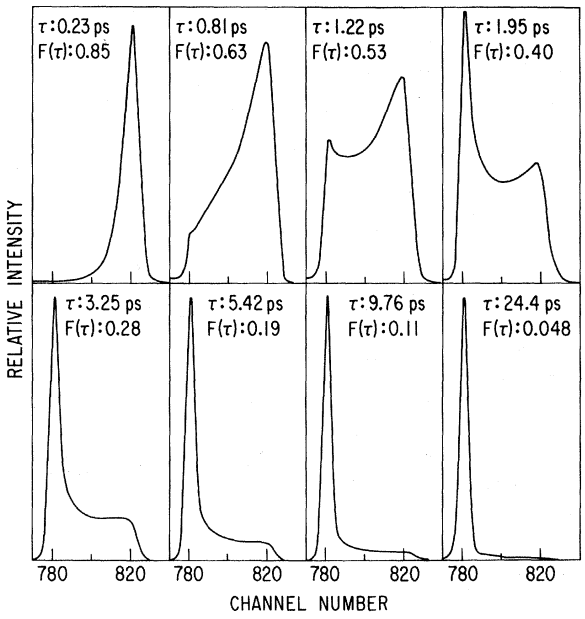

FIG. 2. Hypothetical Doppler line shapes as a function of assumed mean lifetime. $F(\tau)$ is the ratio of the average Doppler shift to the full shift for recoil into vacuum. These line shapes were calculated for a Mg backing as explained in the text, and correspond to a measurement at $\theta_\gamma=0°$ of the 517-keV γ ray deexciting the 2468-keV level of ^{36}Cl. The reaction is ^{2}H(^{35}Cl, $p\gamma$)^{36}Cl with $v/c=5.5\%$, $v/v_0=7.60$, corresponding to $\Delta E=28.6$ keV. The dispersion is 0.66 keV/channel and the detector resolution is 3.3 keV FWHM.

in the determination of the background.

The fitting procedure consisted of fixing the detector response and the ΔV and dE/dx parameters and varying τ to obtain a χ^2 versus τ plot. For each case the curve exhibited a single minimum from which the best value of τ was extracted for the backing material and detector angle in question. An example of the variation of the line shape with τ is shown in Fig. 2.

IV. RESULTS

A. $^2H(^{18}O,p)^{19}O$

γ rays were observed from the $^2H(^{18}O, n\gamma)^{19}F$ ($Q = 5.77$ MeV) and $^2H(^{18}O, p\gamma)^{19}O$ ($Q = 1.73$ MeV) reactions and also from $^{19}O(\beta^-)^{19}F$. The 1376-keV ^{19}O $2 \rightarrow 1$ transition, corresponding to the decay of the second excited state at 1471.3 ± 0.9 keV[16] to the first excited state at 96.0 ± 0.5 keV,[16] was the only transition studied. Portions of the three 0° spectra showing this transition are illustrated in Fig. 3. In addition to the ^{19}O 1376-keV γ rays, γ-ray peaks are identified with ^{19}F transitions which follow the β^- decay of ^{19}O to the fifth excited state of ^{19}F at 1554 keV. The ^{19}F $5 \rightarrow 2$ transition provided a convenient energy reference (1356.9 ± 0.3 keV)[16] and a good measure of the detector resolution (2.7-keV FWHM). A portion of the γ-ray energy region near the upper end of the Doppler-broadened ^{19}O 1376-keV line was obscured by the ^{19}F $5 \rightarrow 1$ transition, and so was not included in the analysis of this line shape. The spectrum from the target on the Mg backing also contained a contribution from the ^{24}Mg $1 \rightarrow 0$ transition which arose mostly from Coulomb excitation, with a small contribution from the ^{24}Na β^- decay to the second excited state of ^{24}Mg. (The apportionment to these two sources was carried out utilizing the intensity of the ^{24}Mg $2 \rightarrow 1$ transition.) The ^{24}Mg $1 \rightarrow 0$ Coulomb-excitation line shape was generated (the dashed line in the bottom spectrum of Fig. 3) and subtracted with negligible error since this line shape is quite well understood.[15] After subtraction of the assumed backgrounds (solid and dashed curves of Fig. 3), the 0° line shapes are as given in Fig. 4. Unfortunately, these line shapes contain an unknown contribution from the $^2H(^{18}O, n)^{19}F$ $(5 \rightarrow 2)$ transition. The lifetime of the fifth excited state of ^{19}F is fast enough (~4.4 fsec[16]) so that this transition will show essentially the full kinematical Doppler shift and the reaction is exothermic so the γ-ray peak will be Doppler broad-

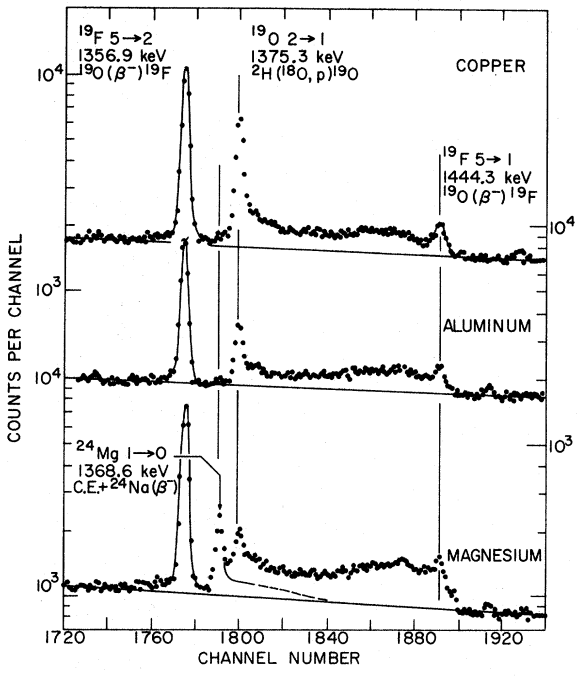

FIG. 3. Partial 0° γ-ray spectra from the bombardment of ^2H by ^{18}O. The line shape of the ^{19}O $2 \rightarrow 1$ transition for the ^{19}O recoils decaying in Cu, Al, and Mg backings are indicated as are the peaks from $^{19}O(\beta^-)^{19}F$ and the Coulomb excitation of ^{24}Mg.

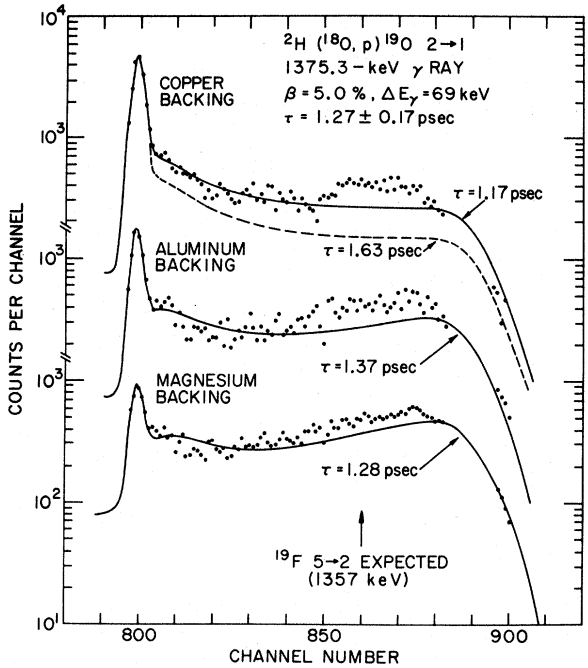

FIG. 4. The line shapes of Fig. 3 with background subtracted. The solid curves are best fits as explained in the text. The excess counts centered near channel 860 are believed to be due to the Doppler broadened ^{19}F $5 \rightarrow 2$ transition as discussed in the text.

ened. Its expected position is indicated in Fig. 4. Because of the possible presence of this transition, the least-squares line-shape fits were restricted to the energy regions corresponding to channels 790 to 840, with the results shown by the solid curves of Fig. 4. Clearly there is evidence for a surplus of counts in the region where the ^{19}F $5 \rightarrow 2$ transition is expected, with a distribution consistent with the expected Doppler broadening. The lifetimes corresponding to the "best" fits (i.e., minimum χ^2) are indicated. The three values agree within the uncertainties and an average value of 1.27 ± 0.17 psec is adopted for the lifetime of the ^{19}O second excited state. Fits were also made to all the data points of Fig. 4. In this case the average value for the lifetime was 1.16 ± 0.14 psec. It appears that the uncertainty in the relative intensity of the ^{19}F $5 \rightarrow 2$ transition introduces little error in the result for the ^{19}O lifetime.

The energy of the ^{19}O $5 \rightarrow 2$ transition was measured to be 1375.3 ± 0.5 keV. Using 96.0 ± 0.5 keV[16] for the excitation energy of the first excited state results in an excitation energy of 1471.4 ± 0.7 keV for the second excited state of ^{19}O in excellent agreement with previous results.[16]

The line shapes recorded at 30 and 60° to the beam were also analyzed. As discussed in Sec. III, the line shapes, especially those taken at 60°, were subject to a large smearing effect due to the angular acceptance angle of ±13°, and the Gaussian-smearing method of simulating this effect was too crude to handle well such a large effect. This was reflected in poorer fits than for the 0° data; nevertheless, the lifetimes obtained for the minimum χ^2 were in excellent accord with the 0° results.

There have been two recent determinations of the lifetime of the ^{19}O 1471-keV level, both using the DSAM. The first[17] utilized the ^{18}O$(d,p)^{19}$O reaction and observed the Doppler line shape of the 1376-keV γ rays in an $H_2{}^{18}O$ ice target. The result for the mean lifetime of 1.22 ± 0.36 psec is in excellent agreement with the present result. The second[18] utilized the inverse ^{2}H$(^{18}\text{O},p)^{19}$O reaction at an ^{18}O energy of 27 MeV and a 200-μg/cm^2 titanium layer loaded with deuterium. The backing was copper. In other words, the experimental procedure was very similar to the present one for the Cu backing; the main differences were that the detector resolution was 5.5 keV FWHM (about twice our resolution) and data at 45, 60, 120, and 135° to the beam were used rather than 0° data as in the present work. A mean lifetime of 1.80 ± 0.29 psec was obtained in rather poor agreement with the present result of 1.27 ± 0.17 psec. The line shape for $\tau = 1.63$ psec shown for the Cu-backing data in Fig. 4 gives an indication of the discrepancy.

B. ^{2}H$(^{19}\text{F},p)^{20}$F

The bombardment of deuterium by a ^{19}F beam produced only one γ-ray transition which could be easily used to deduce a lifetime by the present method. This was the ground-state decay of the 656-keV first excited state of ^{20}F formed via the ^{2}H$(^{19}\text{F},p)^{20}$F reaction which has a Q value of 4.373 MeV. The second excited state at 823 keV has a lifetime of 79 ± 6 psec[19] which is outside our range of measurement. The third excited state at 984 keV was quite weakly formed and γ rays corresponding to the main decay mode, 90% to the ground state, were obscured by Coulomb excitation of the 983-keV first excited state of ^{48}Ti. The fourth excited state at 1057 keV was strongly formed and its ground-state decay (~100%[20]) clearly observable. However, the mean lifetime was observed to be very fast compared to the stopping time in the three targets, so that a line-shape analysis was not possible. A comparison of the centroid of the 1057-keV peak as observed with the Mg-, Al-, and Cu-backed targets yielded 22 fsec for the mean lifetime. However, this result is extremely approximate, since the traversal time of the ^{20}F ions in the 200-μg/cm^2 targets is ~30 fsec, and so our assumption that the reaction takes place midway through the target introduces considerable error, as does our inexact knowledge of the target density. We consider our observations for this level to be consistent with the previously measured mean lifetime of 45 ± 13 fsec.[21]

Line shapes were extracted from the 0° spectra only. The other spectra were taken for survey purposes and to examine the background underlying the ^{20}F 646-keV peak. The three 0° line shapes obtained after background subtraction are shown in Fig. 5. Only the pulse-height region between channels 1036 to 1080 was used in the analysis. The region above channel 1080 was obscured by the ^{72}Ge 691-keV distribution from inelastic neutron scattering in the detector. The region below channel 1036 is dominated by the 656-keV stopped peak resulting from the 64% branch of the (79 ± 6)-psec 823-keV level to the 656-keV level. In addition, the pulse-height region between channels 1049 and 1064 was weighed out of the least-squares fit in the Cu-backed spectrum, since the ^{63}Cu $1 \rightarrow 0$ transition (669 keV), produced via Coulomb excitation, was observed in this region in the 120° spectrum.

It was assumed that feeding from higher states has negligible effect on the region of the line shape which was fitted. The only ^{20}F states with known branches to the 656-keV level are the 823-keV level already discussed and the 984- and

1044-keV levels,[20] which have branches of 10 and 80%, respectively, to the first excited state. The 984-keV level with a lifetime of 1.8 ± 0.4 psec[21] is formed too weakly to influence our result (the 984 → 656 transition was not observed) and the 2044-keV level, also formed weakly, has a lifetime of 37 ± 16 fsec[21] so that feeding from it will cause negligible error.

The solid curves of Fig. 5 show the theoretical fits calculated in each case for the indicated value of τ. We reiterate that the region of the stopped peak at ~ channel 1030 was excluded from the fitting procedure: The solid curves in this region, therefore, illustrate the considerably lesser magnitude of the "stopped component" due solely to the 656-keV lifetime. The intensity of the stopped component due to feeding via the 823-keV level is given by the dashed curves in Fig. 5 with the solid curves as background. The ratio of this intensity to the total line-shape intensity should then be independent of the stopping material. This ratio was found to be 0.145, 0.153, and 0.161 for Mg, Al, and Cu, respectively. These ratios agree fairly well within the estimated uncertainty of ±0.01. The lifetimes extracted for the three backings are in fair agreement, and we adopt the value 0.42 ± 0.05 psec for the average. This result is in excellent agreement with the two previous values of 0.37 ± 0.06 psec[21] and 0.36 ± 0.08 psec.[22]

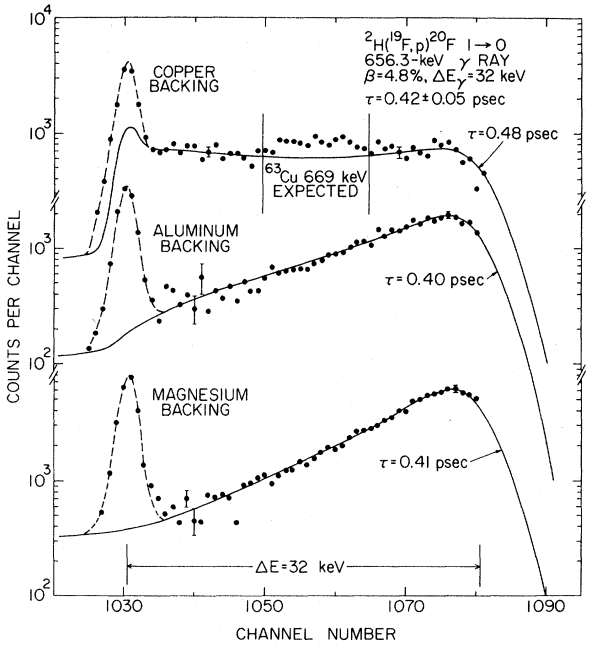

FIG. 5. Partial 0° γ-ray spectra from the bombardment of ^{2}H by ^{19}F illustrating the ^{20}F 1→0 line shape. Background has been subtracted, except for the ^{63}Cu 1→0 transition (upper spectrum) from Coulomb excitation of the backing. The solid curves are the best fits to the region between channels 1036–1080 as explained in the text.

C. ^{2}H(^{32}S,p)^{33}S and ^{2}H(^{32}S,n)^{33}Cl

Several DSAM studies of lifetimes of ^{33}S levels have recently been made.[23–26] All of these agree that of the seven levels below 3.80 MeV excitation in ^{33}S only the first excited state at 840.91 ± 0.05 keV[27] has a lifetime in the range $0.25 \leq \tau \leq 10$ psec which we consider appropriate for the present method. Of these first seven levels only the third and seventh have detectable branches to the first excited state and both these levels have lifetimes faster by a factor of $\gtrsim 10$ than the first excited state[23–26]; thus, we can measure the lifetime of the first excited state of ^{33}S in a singles measurement. Since ^{33}Cl and ^{33}S form a mirror pair we expect the above remarks to hold for ^{33}Cl also. No lifetimes have been previously determined for ^{33}Cl. The Q values leading to ^{33}S and ^{33}Cl are 6.417 and 0.07 MeV, respectively.

Spectra were recorded at 0, 45, and 90° to the

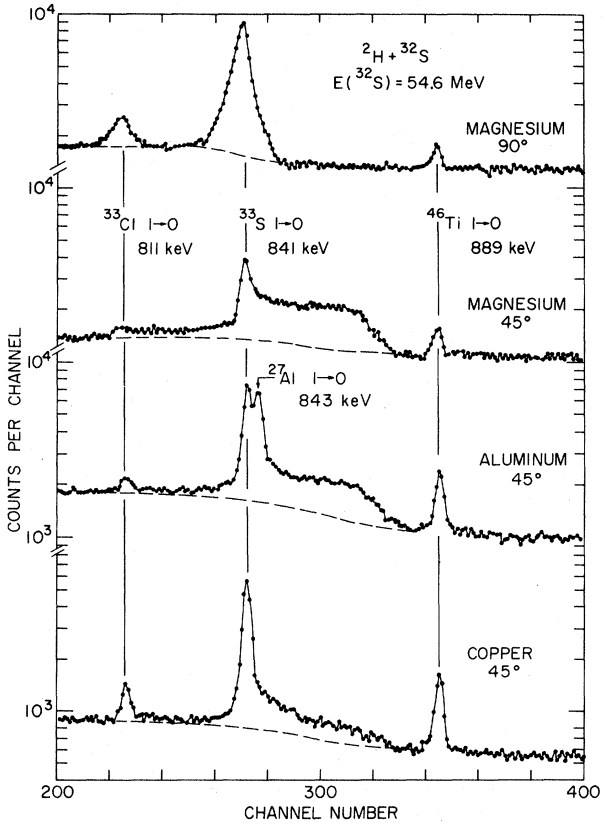

FIG. 6. Partial γ-ray spectra for ^{2}H + ^{32}S showing the line shapes of the ^{33}Cl and ^{33}S 1→0 transitions.

beam for all three backings. Portions of all three of the 45° spectra and also the 90° spectra for the magnesium-backed target are illustrated in Fig. 6. It is seen that the ^{33}Cl $1 \rightarrow 0$ transition is weak relative to the ^{33}S $1 \rightarrow 0$ transition. Spectra were taken at 64-, 72-, and 76-MeV ^{32}S energy as well as at 54.6 MeV with no improvement in the ratio of ^{33}Cl and ^{33}S $1 \rightarrow 0$ transition yields. Since the full kinematic Doppler shift for the ^{33}Cl 810.51 $\pm$ 0.16-keV[27] transition is 32.6 keV at 45°, the γ-ray distribution for this transition runs into that for the ^{33}S 841-keV transition. The overlap of the two line shapes is worse for the 0° spectra and in both cases the background under the ^{33}Cl line shape was difficult to ascertain. Thus a line-shape analysis was not carried out for this transition. Instead, for both the ^{33}Cl and ^{33}S transitions, the intensity of the stopped peak was extracted and an analysis of this intensity as a function of the stopping time of the recoiling ions was made. This method,[28,29] which is similar in concept to a recoil distance measurement,[1] gives the decay curves illustrated in Fig. 7. The three target backings give stopping times (t_s) in the ratio ~3 : 2 : 1 for Mg : Al : Cu. For each target backing there are two points, one for 45° and one for 0°, since slightly different pulse-height regions were included in the sum over the stopped peak for the two spectra and thus the appropriate values of t_s are different. This is so because t_s is the time required to reach some final (small) velocity, whose value is determined by the maximum γ-ray energy (or corresponding recoil velocity) included in the above sum. For the ^{33}S $1 \rightarrow 0$ transition there are no Al-backing data, since the ^{27}Al $1 \rightarrow 0$ transition, due to Coulomb excitation, obscured these data (see Fig. 6). For both transitions a point for $t_s = 0$ was obtained from 90° spectra, i.e., the total intensity corresponds to $t_s = 0$. Note that the first excited states of ^{33}S and ^{33}Cl have $J^\pi = \frac{1}{2}^+$ so there are no angular distribution or correlation effects. The mean lifetimes given in Fig. 7 result from least-squares fits to the slopes of the two decay curves.

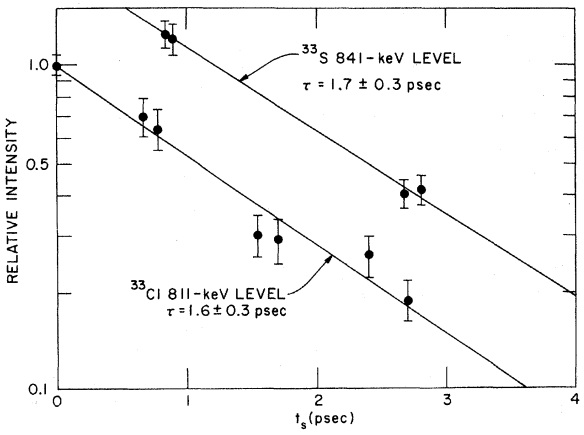

FIG. 7. Decay curves for the first excited states of the mirror pair ^{33}Cl and ^{33}S. t_s is the time needed for the recoiling ions to slow to a certain (small) final velocity. There are two experimental points (from the 0 and 45° spectra) for each backing material. The indicated mean lives result from least-squares fits to the data.

A line-shape analysis of the ^{33}S $1 \rightarrow 0$ transition was also made on the 0 and 45° data for the Mg- and Cu-backed targets. The Cu backing gave an average of 2.2 $\pm$ 0.3 psec while the Mg backing gave an average of 1.8 $\pm$ 0.3 psec. We take 2.0 $\pm$ 0.3 psec for the result of the line-shape analysis. Since this result is more reliable than that from the "decay-curve" method we adopt 2.0 $\pm$ 0.3 psec for our final lifetime for the ^{33}S first excited state. Then, since we believe the lifetime ratio obtained from the "decay-curve" comparison is more accurate than the individual results, we take 1.8 $\pm$ 0.3 psec as our final value for the lifetime of the ^{33}Cl first excited state.

D. ^{2}H(^{34}S, p)^{35}S and ^{2}H(^{34}S, n)^{35}Cl

In the study of these reactions γ-ray spectra were recorded at 0° to the beam for all three targets. Some data were also taken at angles of 55, 90, and 120°. From the 0° data line shapes were extracted for γ-ray peaks corresponding to the ground-state decays of the first two excited states of ^{35}Cl and the ^{35}S 1574 $\rightarrow$ 0 and 2350 $\rightarrow$ 1574 transition.[30] Analysis of these line shapes yielded the results collected in Table III.

Both the ^{35}Cl lifetimes were obtained assuming negligible influence from feeding via higher-lying levels. This assumption was based on previous γ-ray branching ratio and lifetime measurements[31-34] and on the relative γ-ray intensities observed in the present work. Likewise, for the ^{35}S 2350-keV level, there was no evidence in the present results for any feeding from states with lifetimes long enough to influence the line shape. The line shape of the 2350 $\rightarrow$ 0 transition, which has a branching ratio of 73%,[30] was obscured by another γ-ray peak of unknown origin and shape. Thus the results for the 2350-keV level are based on the 776-keV branch (of 27%) to the 1574-keV level. The line shape obtained at 0° using the Cu-backed target was partially obscured by a contribution from Coulomb excitation of the ^{65}Cu 770-keV first excited state and so was not analyzed.

From the relative intensities of the 776-keV line and the 1574-keV line it was determined that the

TABLE III. Résumé of results from $^{2}H+^{34}S$.

Nucleus	Level (keV)	Mean lifetime (psec) Mg backing	Al backing	Cu backing	Average
^{35}Cl	1219	0.28±0.05	0.29±0.05	0.31±0.06	0.29±0.04
^{35}Cl	1762	0.57±0.08	0.54±0.07	0.53±0.08	0.54±0.07
^{35}S	1574	2.8 ±0.4	3.8 ±0.6	>3.0	3.3 ±0.5
^{35}S	2350	1.34±0.20	1.24±0.20		1.3 ±0.2

1574-keV line was fed 17% via the 2350-keV level. This feeding fraction and the lifetime of the 2350-keV level were used in the analysis of the 1574-keV line shape.

E. $^{2}H(^{35}Cl,p)^{36}Cl$ and $^{2}H(^{35}Cl,n)^{36}Ar$

These two reactions have Q values of 6.352 and 6.282 MeV, respectively. Spectra were recorded at 90, 55, and 0° to the beam with the Mg backing and at 0° to the beam with the Cu backing, all for $E_\gamma < 2.6$ MeV. Only this cursory survey was made, because it was immediately clear that there was a very rich source of measurable lifetimes which should be studied in detail and with the aid of coincidence techniques.

To illustrate, previous DSAM work on ^{36}Ar lifetimes[35] includes lower limits of 2, 1, 1, and 0.6 psec for the mean lifetimes of levels at excitation energies of 4178, 4978, 5171, and 5897 keV. We observed the 4178 → 1970 transition and possibly the 4978 → 4178, 5171 → 4178, and 5897 → 4178 transitions. The two-escape peak of the 4178 → 1970 transition and a 796-keV transition which may possibly be the 4978 → 4178 transition are displayed in Fig. 8. For neither of these transitions can we see any Doppler effects and from an analysis similar to that used to obtain the "decay curve" of

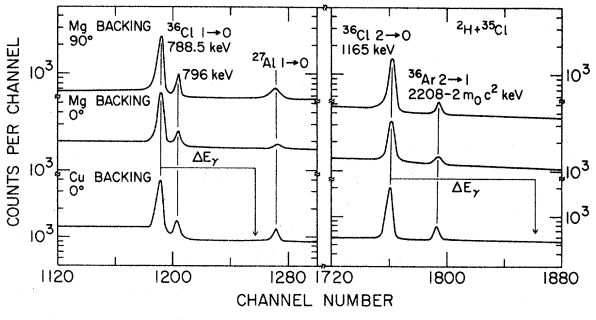

FIG. 8. Partial γ-ray spectra from $^{2}H+^{35}Cl$. None of the four peaks from ^{36}Cl and ^{36}Ar exhibit any discernible Doppler effects so that mean lives long compared to the stopping time are indicated.

Fig. 7 we obtain the limit $\tau > 3$ psec for the 4178-keV level. In setting this limit, allowance was made for feeding of the 4178-keV level by higher-lying long-lived states. A similar limit applies to the 4978-keV level if, in actual fact, the 796-keV line is to be associated with its decay. The assignment of a 993-keV peak to the ^{36}Ar $5^- \rightarrow 3^-$ 5171 → 4178 transition can be made with more confidence. If this assignment is correct, then a limit $\tau > 3$ psec can safely be set for the 5171-keV level. It is clear that without coincidence measurements or perhaps a knowledge of the relative feeding of the ^{36}Ar states in the (d, n) reaction, it is not possible to rigorously assign γ-ray peaks to particular cascades in ^{36}Ar. When this is done it would seem that there are several lifetimes in ^{36}Ar which can be measured by the recoil distance technique.

The assignment of γ-ray peaks to ^{36}Cl also was difficult. The ground-state decays of the first and second excited states of ^{36}Cl at 788.46±0.20 keV[36] and 1164±2 keV[36] were both observed as illustrated in Fig. 8. Neither full-energy peaks showed any Doppler effects and we set limits of 5 and 3 psec, respectively, for the two lifetimes. Again a recoil distance measurement is indicated.

From qualitative examination of the line shape of its ground-state decay, it is clear that the ^{36}Cl 1951-keV level (fourth excited state) has $\tau > 1$ psec. Similarly, the 1959-keV level (fifth excited state) has $\tau < 0.8$ psec. More cannot be said, since these two line shapes were unresolved from that of the ^{36}Ar 1 → 0 transition.

One line shape which yielded a definite level lifetime was that for the ^{36}Cl 6 → 4 transition shown in Fig. 9. The γ-ray energy was measured to be 517.4±0.4 keV. The assignment to the decay of the ^{36}Cl 2468-keV level is based on $^{35}Cl(n,\gamma)^{36}Cl$ branching ratios[36] and on the observation of the same line (516±1 keV) following bombardment of ^{34}S by a 3.2-MeV triton beam. Since ^{36}Cl, but not ^{36}Ar, can be formed by this means, we have eliminated the possibility that the γ ray originates in ^{36}Ar. The values for the mean lifetime resulting from analysis of the three line shapes of Fig. 9

were in excellent agreement. We adopt the average $\tau = 1.50 \pm 0.18$ psec for the ^{36}Cl 2468-keV level.

F. ^{2}H(^{37}Cl, p)^{38}Cl

Our results from the bombardment of ^{2}H with ^{37}Cl are from a rather rough survey run with just barely adequate statistics and for $E_\gamma \lesssim 1300$ keV only. Nevertheless, two ^{38}Cl lifetimes were extracted from 90, 55, and 0° spectra recorded for all three target backings. A decay scheme[3] for ^{38}Cl is shown in Fig. 10. The γ-ray line shapes studied were those of 308 and 364 keV, corresponding to the 1617 → 1309 and 1981 → 1617 transitions, respectively. The 0° line shapes were analyzed with the results shown in Fig. 11. In both cases the lifetimes obtained from the three backings are in agreement. The adopted averages are 2.20 ± 0.20 and 0.56 ± 0.08 psec for the 1617- and 1981-keV levels, respectively.

For the 1981-keV level there is no evidence for feeding from higher long-lived states with $E_x < 2.75$ MeV[3] and no uncertainty was assumed from this source. The 1617-keV level is partially formed by a 12% branch from the 2743-keV level ($\tau \leq 0.03$ psec[3]) and a 31% branch from the 1981-MeV level studied in the present work. The former feeding introduces negligible uncertainty but the latter must be taken into account. The fraction of feeding of the 1617-keV level via the 1981-keV level was easily and accurately calculable from the relative intensities of the 308- and 364-keV γ rays and the branching ratio of the 308-keV 1617 → 1309 transition ($51 \pm 2\%$[3]). The result was found to be $f = 0.213$ with a 7% uncertainty. This fraction and the lifetime of the 1981-keV level were then additional input information in the line-shape analysis of the 308-keV 1617 → 1309 line shape.

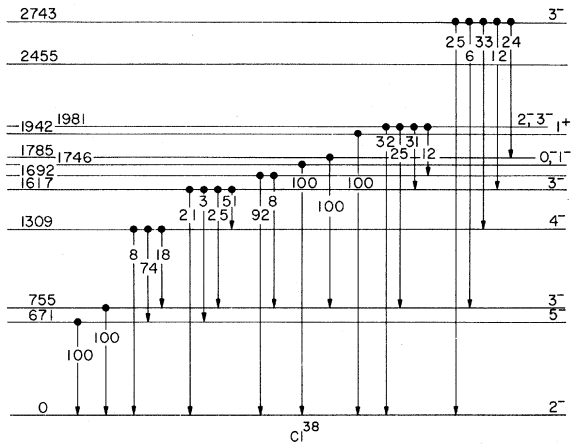

FIG. 10. Decay scheme for the low-lying levels of ^{38}Cl (from Ref. 3).

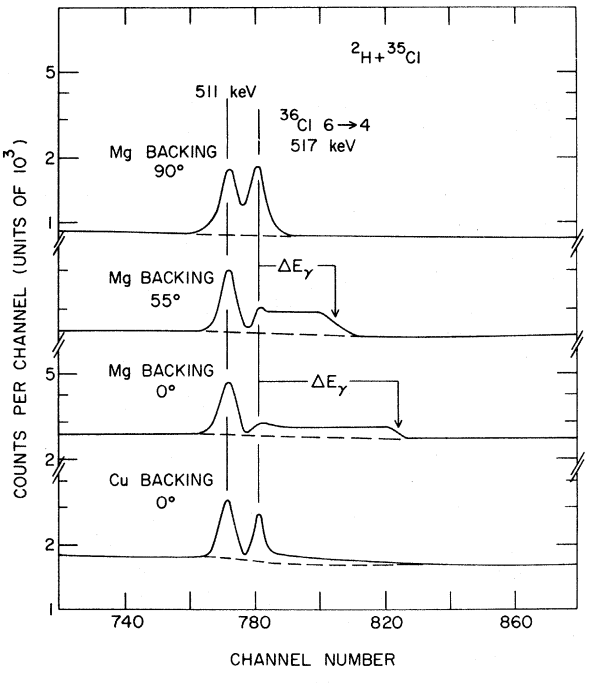

FIG. 9. Partial γ-ray spectra from ^{2}H + ^{35}Cl illustrating the line shape of the ^{36}Cl 6 → 4 transition. From the line shapes of Fig. 2 it is evident that the mean life of the ^{36}Cl 2468-keV sixth excited state is between 1.2 and 2.0 psec. The final average value for the three backings was 1.50 ± 0.18 psec.

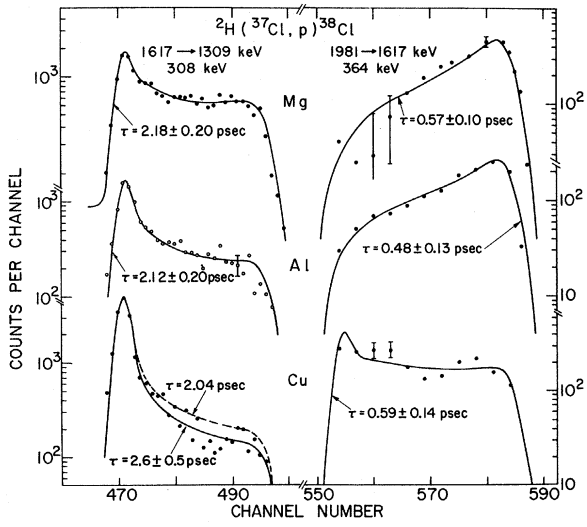

FIG. 11. Line shapes with background subtracted, from 0° γ-ray spectra following bombardment of ^{2}H with ^{37}Cl. The dashed curve for the 308-keV line shape with the Cu backing is given to illustrate the sensitivity to τ.

V. DISCUSSION

Our results are listed in Table IV where they are compared to previous measurements. A perusal of Table IV shows that the uncertainties we have assigned are small compared to previous work. This reflects the rather good statistics of singles measurements and the fact that each of our values is an average of measurements with two or three backing materials. There are no serious disagreements with previous work except for those cases, such as the ^{35}Cl 1219-keV level, where a discrepancy already appeared to exist.

TABLE IV. Résumé of results.

Nucleus	Level (keV)	Mean lifetime (psec) Present	Previous	References
^{19}O	1471	1.27 ± 0.17	1.22 ± 0.36	17
			1.80 ± 0.29	18
			0.90 ± 0.23	a
^{20}F	656	0.42 ± 0.05	0.37 ± 0.06	21
			0.36 ± 0.08	22
^{33}S	841	2.0 ± 0.3	$1.8 < \tau < 5.4$	26
			$1.73^{+1.1}_{-0.45}$	23
			$0.9^{+0.5}_{-0.4}$	25
			1.81 ± 0.36	24
^{33}Cl	811	1.8 ± 0.3	>1.0	b
^{35}S	1574	3.3 ± 0.5	≥1.8	30
	2350	1.3 ± 0.2	0.8 ± 0.2	30
^{35}Cl	1219	0.29 ± 0.04	$0.21^{+0.10}_{-0.08}$	33
			$0.27^{+0.19}_{-0.10}$	31
			0.3 ± 0.1	c
			$0.13^{+0.03}_{-0.02}$	d
			0.215 ± 0.075	34
	1762	0.54 ± 0.07	0.55 ± 0.15	33
			$1.15^{+0.45}_{-0.63}$	31
			0.6 ± 0.2	c
			0.205 ± 0.075	34
^{36}Cl	788	>5	···	
	1164	>3	···	
	2468	1.50 ± 0.18	···	
^{36}Ar	4178	>3	>2	35
^{38}Cl	1617	2.20 ± 0.2	$2.3^{+2.3}_{-0.9}$	3
	1981	0.56 ± 0.08	0.43 ± 0.09	3

[a] F. Hibou, P. Fintz, B. Rastegar, and A. Gallman, Nucl. Phys. A171, 603 (1971).

[b] L. A. Alexander and F. W. Prosser, Jr., Bull. Am. Phys. Soc. 15, 600 (1970).

[c] E. C. Booth and K. A. Wright, Nucl. Phys. 35, 472 (1962).

[d] J. H. Hough and W. L. Mouton, Nucl. Phys. 76, 248 (1966).

Where a lifetime had previously been measured, comparison to theoretical predictions have also been made in the references cited in Table IV. However, for the five new values of τ (two of them lower limits) listed in Table IV some discussion of theoretical predictions is in order.

The ^{33}Cl $1 \rightarrow 0$ transition is found to have a lifetime close to that of its mirror transition in ^{33}S and is thus consistent with the expectation that $B(M1)$ values of mirror decays be approximately equal.[37,38]

Our value of 3.3 ± 0.5 psec for the lifetime of the first excited state of ^{35}S is in fair agreement with the shell-model prediction of 1.4 psec made by Wiechers and Brussaard.[39] It would also be interesting to include in this comparison the recent quite extensive calculations of Wildenthal *et al.*,[40] but these authors do not quote the $B(M1)$ and $B(E2)$ values corresponding to the wave functions they calculated for ^{35}S.

Our lower limit of 5 psec for the ^{36}Cl $1 \rightarrow 0$ transition is already slower than the shell-model prediction[39] of 1.3 psec so that a sizable discrepancy is possible here. On the other hand, the predicted lifetime for the ^{36}Cl $2 \rightarrow 0$ transition is consistent with our lower limit of 5 psec for this level. The ^{36}Cl 2468-keV level is stated[36] to have $J^{\pi} = 3^-$, and it decays to the 2^+ 1949-keV level. Our mean-life of 1.5 psec therefore corresponds to 4.2×10^{-3} single-particle Weiskopf units (W.u.) which is just about of average strength.[38]

The advantages of the "inverse" reaction in DSAM measurements were dwelt on in Sec. I. The disadvantages become obvious when one reviews the present work. Most importantly we find that the background under the line shapes can be sizable and difficult to determine accurately, even when it exhibits no noticeable structure; and all too often there is structure which interferes with the desired line shape. Almost as troublesome is the necessary reliance on auxiliary branching ratio and lifetime information which is often required before a given line shape can be interpreted. This, of course, results from the sensitivity of the method to feeding from higher states with nonnegligible lifetimes. These limitations keep the "inverse" singles type of DSAM measurement from being very widely applicable. However, at its best it is probably the most accurate of the various applications of the DSAM.

ACKNOWLEDGMENTS

We would like to thank H. R. Hyder and K. W. Jones for their expert advice and assistance with the ion sources.

†Work performed under the auspices of the U. S. Atomic Energy Commission.

*Present address: Robert Van de Graaff Laboratorium, Utrecht, The Netherlands.

‡Summer visitor, 1970. Permanent address: Chalk River Nuclear Laboratories, Chalk River, Canada.

[1]See A. Z. Schwarzschild and E. K. Warburton, Ann. Rev. Nucl. Sci. 18, 265 (1968), for a review of the measurement of nuclear lifetimes and in particular for references on methods utilizing the Doppler effect.

[2]A. E. Litherland, M. J. L. Yates, B. M. Hinds, and D. Eccleshall, Nucl. Phys. 44, 220 (1963).

[3]G. A. P. Engelbertink and J. W. Olness, Phys. Rev. C 5, 431 (1972).

[4]L. C. Northcliffe and R. F. Schilling, Nucl. Data A7, 233 (1970).

[5]S. Dushman, *Scientific Foundations of Vacuum Technique* (Wiley, New York, 1962), pp. 544–6.

[6]See e.g., E. K. Warburton, D. E. Alburger, and G. A. P. Engelbertink, Phys. Rev. C 2, 1427 (1970).

[7]E. K. Warburton, D. E. Alburger, and D. H. Wilkinson, Phys. Rev. 129, 2180 (1963).

[8]E. K. Warburton, J. W. Olness, and A. R. Poletti, Phys. Rev. 160, 938 (1967).

[9]N. Bohr, Kgl. Danske Videnskab. Selskab, Mat.-Fys. Medd. 18, No. 8 (1948).

[10]D. I. Porat and K. Ramavataram, Proc. Roy. Soc. (London) A252, 394 (1959); Proc. Phys. Soc. (London) 77, 97 (1961); 78, 1135 (1961).

[11]W. Booth and I. S. Grant, Nucl. Phys. 63, 481 (1965).

[12]A. Van Wijngaarden and H. E. Duckworth, Can. J. Phys. 40, 1749 (1962); J. H. Ormrod and H. E. Duckworth, *ibid.* 41, 142 (1963); J. H. Ormrod, J. R. MacDonald, and H. E. Duckworth, *ibid.*, 43, 225 (1964); J. R. MacDonald, J. H. Ormrod, and H. E. Duckworth, Z. Naturforsch. 21, 130 (1966).

[13]B. Fastrup, P. Hvelplund, and C. A. Sautter, Kgl. Danske Videnskab. Selskab, Mat.–Fys. Medd. 35, No. 10 (1966); P. Hvelplund and B. Fastrup, Phys. Rev. 165, 408 (1968); B. Fastrup, A. Borup, and P. Hvelplund, Can. J. Phys. 46, 489 (1968); P. Hvelplund, Kgl. Danske Videnskab. Selskab, Mat.–Fys. Medd. 38, No. 4 (1971).

[14]O. Haüsser, D. Pelte, T. K. Alexander, and H. C. Evans, Can. J. Phys. 47, 1065 (1969).

[15]D. Schwalm, G. A. P Engelbertink, J. W. Olness, and E. K. Warburton, to be published.

[16]F. Ajzenberg-Selove, Nucl. Phys. A190, 1 (1972).

[17]R. E. McDonald, J. A. Becker, A. D. W. Jones, and A. R. Poletti, Phys. Rev. C 4, 377 (1971).

[18]C. Broude, U. Karfunkel, and Y. Wolfson, Nucl. Phys. A161, 241 (1971).

[19]J. G. Pronko and R. W. Nightingale, Phys. Rev. C 4, 1023 (1971).

[20]P. A. Quin, G. A. Bissinger, and P. R. Chagnon, Nucl. Phys. A155, 494 (1970).

[21]T. Holtebekk, R. Strømme, and S. Tryti, Nucl. Phys. A142, 251 (1970).

[22]R. L. Hershberger, M. J. Wozniak, and D. J. Donahue, Phys. Rev. 186, 1167 (1969).

[23]G. Van Middelkoop and G. A. P. Engelbertink, Nucl. Phys. A138, 601 (1969).

[24]F. Brandolini and C. Signorini, Phys. Letters 30B, 342 (1969); F. Brandolini, J. Benuzzi-Martins, R. A. Ricci, and C. Signorini, Nuovo Cimento Suppl. 2, 600 (1969).

[25]J. E. Cummings and D. J. Donahue, Nucl. Phys. A142, 609 (1970).

[26]R. W. Kavanagh, J. S. Merdinger, and N. Schulz, Nucl. Phys. A146, 410 (1970).

[27]K. A. Snover, J. M. McDonald, D. B. Fossan, and E. K. Warburton, Phys. Rev. C 4, 398 (1971).

[28]P. G. Bizzeti, A. M. Bizzeti-Sona, S. Kalbitzer, and B. Povh, Nucl. Phys. A104, 577 (1967).

[29]K. Bharuth-Ram, K. P. Jackson, K. W. Jones, and E. K. Warburton, Nucl. Phys. A137, 262 (1969).

[30]K. S. Burton and L. C. McIntyre, Nucl. Phys. A154, 551 (1970).

[31]D. D. Duncan, K. H. Buerger, R. L. Place, and B. D. Kern, Phys. Rev. 185, 1515 (1969).

[32]B. W. Hooton, O. Haüsser, F. Ingebretsen, and T. K. Alexander, Can. J. Phys. 48, 1259 (1970).

[33]F. Ingebretsen, T. K. Alexander, O. Haüsser, and D. Pelte, Can. J. Phys. 47, 1295 (1969).

[34]R. J. Van Reenen, W. J. Naude, and W. L. Mouton, Nucl. Phys. A183, 651 (1972).

[35]J. P. Thibaud, M. M. Aleonard, D. Crestera, P. Hubert, F. Leccia, P. Mennrath, Compt. Rend. B270, 115 (1970); J. Phys. (Paris) 31, 131 (1970).

[36]P. M. Endt and C. Van der Leun, Nucl. Phys. A105, 1 (1967).

[37]G. Morpurgo, Phys. Rev. 114, 1075 (1959).

[38]E. K. Warburton and J. Weneser, in *Isospin in Nuclear Physics*, edited by D. H. Wilkinson (North-Holland, Amsterdam, 1969).

[39]G. Wiechers and P. J. Brussaard, Nucl. Phys. 73, 604 (1965).

[40]B. H. Wildenthal, E. C. Halbert, J. B. McGrory, and T. T. S. Kuo, Phys. Rev. C 4, 1266 (1971).